# **Evaluating Spatial and Temporal Patterns of Airshed Classification in Thailand Using Object-Based Classification (OBC)**

Woranut Chansury, Pramet Kaewmesri, Viphada Boonlerd, Pakorn Petchprayoon, Kanmanee Sroysonthawornkul, and Peerapat Khaocharoen

Geo-Informatics and Space Technology Development Agency, Bangkok, Thailand woranut@gistda.or.th, paket.kew@gistda.or.th, viphada.boo@gistda.or.th, pakorn@gistda.or.th, kanmanee7@gmail.com, peerapatkhaocharoen@gmail.com

**Keywords:** Airshed Classification, Object-Based Classification (OBC), Digital Elevation Model (DEM), Meteorological Variables, Air Pollution Dispersion, Temporal Patterns

#### Abstract

Fine particulate matter (PM2.5) remains a major public-health concern in Thailand, with seasonal peaks amplified by terrain-induced stagnation. We delineate nationwide airshed regimes by integrating topography with multi-variable meteorology in an object-based workflow coupled to K-means clustering. Monthly composites for 2003–2024 were assembled for digital elevation (DEM), planetary boundary-layer pressure (PBL; proxy for PBL height), 10-m wind speed (WS10), surface pressure (SUR), surface shortwave radiation (SRAD), TMAX/TMIN, vapor pressure (VAP), and precipitation (PPT), harmonized to a common grid and aggregated to objects. Candidate K=2–10 was evaluated; the Elbow criterion supported K=4.

Four physically interpretable clusters emerge—lowland, two transition belts, and highland—monotonically ordered by elevation and accompanied by coherent atmospheric gradients. From lowland to highland, SUR, TMAX, TMIN, VAP, and PPT decline, winds weaken in transition/highland zones, and PBL pressure decreases (consistent with higher PBL tops); SRAD is modestly lower aloft. Seasonality is systematic: November–February features expansion of transition/highland classes into basins under cooler, more stable conditions, whereas during the Southwest monsoon (May–October) transition belts retract as ventilation and wet scavenging strengthen. Despite boundary shifts, cluster identity at fixed locations is highly repeatable.

The zoning provides an operational scaffold for airshed-aware management: targeting monitoring and advisories in transition belts and basin interiors, supporting cross-provincial coordination, and informing regime-conditioned forecasting. Limitations include a dispersion-focused design and reliance on gridded products. Planned extensions will incorporate ventilation capacity (VC=WS10×PBLH), stagnation frequency, and expanded validation (Silhouette/Gap, bootstrap stability, external/temporal holdouts with independent PM2.5).

# 1. Introduction

Particulate matter (PM2.5), with a diameter of less than 2.5 microns, has become a significant environmental concern in Thailand, particularly in major cities like Bangkok and Chiang Mai, as well as rural areas such as Mae Hong Son. In 2023, PM2.5 concentrations increased by 28% compared to 2022, with levels in Chiang Mai reaching 53.4 to 106.4 μg/m³, exceeding WHO standards and posing health risks (IQAir, 2023). Meteorological factors like wind speed, temperature, vapor pressure (VAP), and precipitation play key roles in PM2.5 dispersion. Temperature inversions, which trap pollutants near the surface, are particularly common in winter (OPDC, 2019).

In low- and middle-income countries (LMICs), air quality management often follows political borders, which may not address transboundary pollution. The airshed concept, which defines regions influenced by similar meteorological and pollution factors, offers a more comprehensive framework for managing air quality across political boundaries (Khan et al., 2024). This study aims to delineate regional and local airsheds in Thailand by integrating topographical and meteorological data, addressing geographical and seasonal variations in air quality to improve management strategies. To evaluate the spatial and temporal patterns of airshed classification across Thailand by applying Object-Based Classification (OBC) to monthly meteorological datasets from 2003–2024.

### 2. Literature Review

# 2.1 Airshed Concept and Classification

The airshed concept plays a critical role in air quality management by recognizing that pollution is influenced by meteorological conditions and emission sources that often cross administrative boundaries. Classifying airsheds based on shared climatic, topographic, and emission characteristics enables more targeted and efficient pollution control strategies. This approach is especially valuable in low- and middle-income countries (LMICs), where traditional governance structures limit cross-boundary interventions. By identifying regions with similar air quality profiles, airshed delineation improves hotspot detection and policy implementation (Khan et al., 2024).

# 2.2 Meteorological and Topographical Factors in Air Pollution Dispersion

Meteorological and geographical conditions are key determinants in the dispersion and accumulation of air pollutants. Variables such as wind speed, temperature, precipitation, and air pressure influence how pollutants spread and persist in the atmosphere. Temperature inversions—common in colder months—trap pollutants near the surface, while wind patterns and terrain features like valleys and mountains can create stagnant zones that intensify pollution. These factors are essential for analyzing the spatiotemporal behavior of pollutants and designing effective air quality management strategies (Ghosh et al., 2021; Thitaporn, 2013).

# 2.3 Advancements in Remote Sensing and Object-Based Classification (OBC)

Advancements in remote sensing have significantly enhanced the monitoring of air pollution and environmental variables. High-resolution satellite imagery and sensors now provide precise, real-time data on atmospheric and surface conditions. A key development is object-based classification (OBC), which improves classification accuracy by grouping pixels into meaningful objects based on spatial, spectral, and contextual attributes, rather than analyzing individual pixels. The OBC process typically includes image segmentation, object classification, and spatial analysis.

Mathematically, segmentation is expressed as a function:

$$S(I) \rightarrow O = \{O1, O2, ..., On\}$$
 (1)

where I is the input image a  $O_n$  denotes the resulting image objects

These objects are then classified using techniques such as kmeans clustering or machine learning. In air pollution studies, OBC enables the integration of meteorological, topographical, and pollutant data, supporting more accurate mapping of pollution dispersion patterns.

# 2.4 Air Quality Challenges and Seasonal Health Impacts in LMICs

Air quality management in low- and middle-income countries (LMICs) faces numerous challenges, including limited financial resources, inadequate monitoring infrastructure, and weak enforcement of environmental regulations. These issues are especially pronounced in rapidly growing urban areas where pollution from traffic, construction, and biomass burning is widespread. Despite advances in remote sensing and affordable air monitoring technologies, LMICs often struggle to implement effective air quality strategies due to structural and resource limitations.

Seasonal variations further complicate air pollution management. In many LMICs, PM2.5 concentrations tend to peak during winter and dry seasons due to temperature inversions and increased combustion activities, while rainy seasons generally see reduced levels as precipitation helps remove airborne particles (OPDC, 2019; Pope et al., 2009). These fluctuations have significant health implications. Long-term exposure to PM2.5 is linked to respiratory and cardiovascular diseases, including asthma, chronic bronchitis, lung cancer, and heart disease (Lelieveld et al., 2015). Vulnerable groups such as children, the elderly, and those with pre-existing conditions are particularly at risk.

To address these challenges, LMICs require adaptive and costeffective approaches that integrate seasonal air quality data, enforce emission controls, and promote public awareness. Initiatives such as Clean Air Asia have demonstrated the value of regional collaboration and the use of remote sensing data to improve pollution tracking and policy development. Seasonal patterns in PM2.5 underscore the urgency of targeted interventions during high-risk periods, including public advisories, the adoption of cleaner technologies, and crosssectoral cooperation.

# 3. Datasets use in the study

# 3.1 Topographic Characteristics

Thailand ( $\approx$ 5°–21° N, 97°–106° E;  $\sim$ 513,000 km²) spans coastal lowlands, extensive alluvial plains, inter-montane basins, and high mountain ranges, with elevations from sea level to  $\sim$ 2,565 m. The national climate is tropical monsoon, characterized by a cool–dry season (November–February), a hot pre-monsoon (March–April), and a wet Southwest-monsoon season (May–October). Orography exerts strong control on local ventilation: the Central Plains (e.g., Chao Phraya basin) are predominantly low-lying, while the North and West contain basin-and-range terrain that channels winds and modulates boundary-layer structure.

Basin-like terrains—especially inter-montane basins such as the Chiang Mai–Lamphun basin—are more prone to smog accumulation than adjacent plains, owing to terrain-induced sheltering and frequent air-stagnation under stable conditions in the cool–dry season (WHO, 2016; Phopsuk, 2019). This study therefore treats basin interiors and their rims as candidate airshed hotspots, while still delineating regimes nationwide to support cross-boundary management. Major urban centers (e.g., Bangkok in the coastal/lowland setting and Chiang Mai in a basin setting) provide contrasting dispersion environments that are representative of Thailand's topographic diversity.

To represent terrain with high fidelity across the country, we employed a NASA Digital Elevation Model (DEM) that integrates SRTM, ASTER GDEM v3, and ICESat sources (Crippen et al., 2016). DEM-derived metrics are analyzed jointly with meteorological drivers (e.g., boundary-layer height, wind, precipitation, temperature) to quantify how orography and seasonal monsoon dynamics structure dispersion capacity and, consequently, the spatial patterning of airshed classes.

# 3.2 Meteorological Data

All meteorological predictors were compiled as monthly composites for 2003–2024. Variables include planetary boundary-layer height (PBL), wind speed (WS), surface pressure (SUR), precipitation (PPT), surface shortwave radiation (SRAD), maximum/minimum temperature (TMAX/TMIN), and vapor pressure (VAP). Datasets were harmonized to a common analysis grid and time base; monthly mode values were then aggregated to OBC segments for clustering.

- Planetary Boundary Layer (PBL): The atmospheric layer closest to the Earth's surface, influenced by energy and moisture exchanges. PBL height data from ECMWF are used to identify the vertical extent for PM2.5 dispersion (Simiu et al., 2015).
- Surface Pressure (SUR): Surface-level atmospheric pressure, which influences air flow and circulation patterns (Simiu et al., 2015).

TerraClimate Dataset: This high-resolution (~4 km) global climate dataset provides monthly time series of climate variables including precipitation, radiation, temperature, wind speed, and vapor pressure (Abatzoglou et al., 2018; Araghi et al., 2023).

 Precipitation (PPT): Interpolated using the Climatically Aided Interpolation (CAI) method, integrated with WorldClim data.

- Surface Shortwave Radiation (SRAD): Adjusted using CRU TS4.0 and JRA-55 reanalysis.
- Maximum & Minimum Temperature (TMAX & TMIN): Combined from WorldClim v1.4 and v2.0, CRU TS v4, and JRA-55 (Royal Irrigation Department, 2014).
- Vapor Pressure (VAP): Represents atmospheric moisture content from evapotranspiration.
- Wind Speed (WS): Uses 10-m average wind speed data (Saldanha et al., 2024).

# 4. Methodology

# 4.1 Object-Based Classification (OBC)

Object-based image analysis (OBC) was conducted using eCognition software. Multi-resolution segmentation (MRS) was applied with the following parameters: Scale = 50, Shape = 0.1, and Compactness = 0.5. These parameters were selected to balance thematic (e.g., topographic and climatic) and spatial information during the segmentation process.

The scale parameter, which controls the maximum allowed heterogeneity within image objects, was set to 50 to capture meaningful patterns of elevation and climate zones while avoiding excessive over-segmentation. A low shape weight of 0.1 was used to emphasize spectral/thematic consistencyappropriate in environmental studies where surface variation is driven more by gradients in elevation and climate than by geometric form. The compactness value of 0.5 provides a balance between compact and smooth boundaries, allowing segments to align with natural transitions in terrain and atmospheric features.

These settings align with prior practice; for example, Wang (2018) recommended compactness values between 0.4 and 0.6 to maintain boundary realism in complex landscapes. Low shape weights (  $\!\approx\!0.1\text{--}0.3)$  have likewise been reported as suitable for preserving thematic detail in topographic classification using DEM data (Wang, 2018).

# 4.2 K-Mean Clustering

A K-means algorithm was applied to cluster the integrated DEM and monthly meteorological datasets. Various values of K (2 to 10) were tested to explore spatial and temporal clustering patterns. The optimization aimed to minimize within-cluster distances (Hall & Minns, 1999):

$$J(S:X) = \sum_{i=1}^{c} \sum_{k=1}^{N} d_{ik}^{2} (x_{k}, s_{i})$$
(2)

Where:

I(S:X) = total within-cluster variance

c = number of clusters

N =number of data points

 $x_k$  = data point k  $s_i$  = centroid of cluster  $i_k$   $d_{ik}^2$  = Euclidean distance between  $x_k$  and centroid  $s_i$ 

### 4.3 Cluster Validation

The Elbow Method was employed to determine the optimal number of clusters k This method involves computing the Sum of Squared Errors (SSE) or Total with-cluster sum of squared Euclidean distance for different values of k and identifying the point at which the SSE curve exhibits an "elbow", suggesting that additional clusters provide minimal improvement in model performance.

The SSE for a given value of k is calculated as:

$$SSE = \sum_{k=1}^{k} \sum_{x_i \in S_k} ||x_i c_k||_2^2$$
(3)

Where:

= is the set of points in cluster k $C_k$  = frequency of cluster  $C_i$  over the 12-month period  $X_i$  = total number of unique cluster labels observed

 $\|X_i C_k\|_2^2$  = is the squared Euclidean distance between  $X_i$  and the cluster centroid

### 5. Results and Discussion

# 5.1 Geoclimatic Zoning Analysis

The Result of Elbow Method was employed to determine the optimal number of clusters (K) for this study. Figure 1 presents the Total Within-Cluster Sum of Squares (WCSS) for each tested K value. A noticeable change in the slope of the WCSS curve occurs between K = 4 and K = 5, indicating a significant reduction in WCSS up to K = 4, followed by a more gradual decline. This inflection point, commonly referred to as the "elbow," suggests that K = 4 is the most appropriate choice. Therefore, K = 4 was selected for clustering in this study to ensure more meaningful and accurate results. Elbow analysis indicates a clear inflection at K=4, and qualitative inspection of K>4 partitions shows fragmentation of transition belts without introducing new, physically distinct regimes—supporting K=4 on parsimony and interpretability grounds.

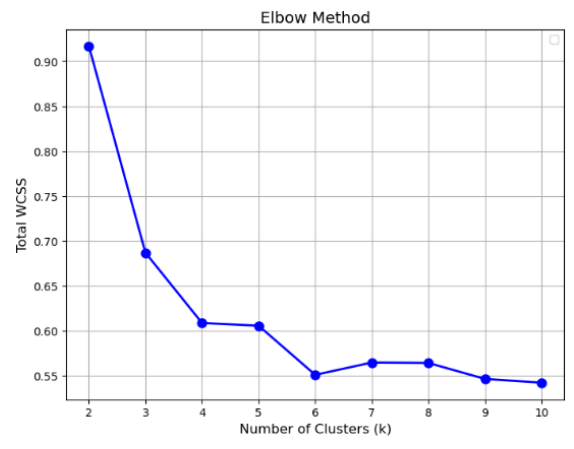


Figure 1. Elbow Method Result

Geoclimatic zones were identified using Object-Based Classification (OBC) in combination with K-means clustering (Hall & Minns, 1999). Monthly mode values of topographic and meteorological variables were used, and the optimal number of clusters was validated using the Elbow Method. Key variables included Digital Elevation Model (DEM) data and meteorological datasets, acknowledging the role of topography in influencing regional climate and ecosystems. As topographic variation directly affects climatic parameters such as temperature, pressure, and precipitation clustering these parameters supports the delineation of geoclimatic zones with environmental significance.

The analysis identified four primary climate zones, showing a clear relationship between elevation and key environmental parameters. As elevation increases, air pressure, temperature, and precipitation generally decrease.

These results confirm the strong influence of elevation on surface pressure, temperature, and vapor pressure. Specifically:

- Surface pressure decreases from 1,006.54 hPa in lowland areas to 934.19 hPa in highland areas due to reduced air density with altitude.
- Temperature shows a declining trend: maximum temperatures fall from 32.37°C to 30.12°C, and minimum temperatures from 23.80°C to 18.73°C.
- Precipitation and vapor pressure also decline with elevation, reflecting reduced humidity and moisture content.

The clusters can be interpreted as follows:

- Cluster 1: Warm, humid lowlands with strong wind circulation.
- Cluster 2 and 3: Transition zones with moderate elevation and intermediate climate characteristics.
- Cluster 4: Highland and mountainous zones with cool, dry conditions and low surface pressure.

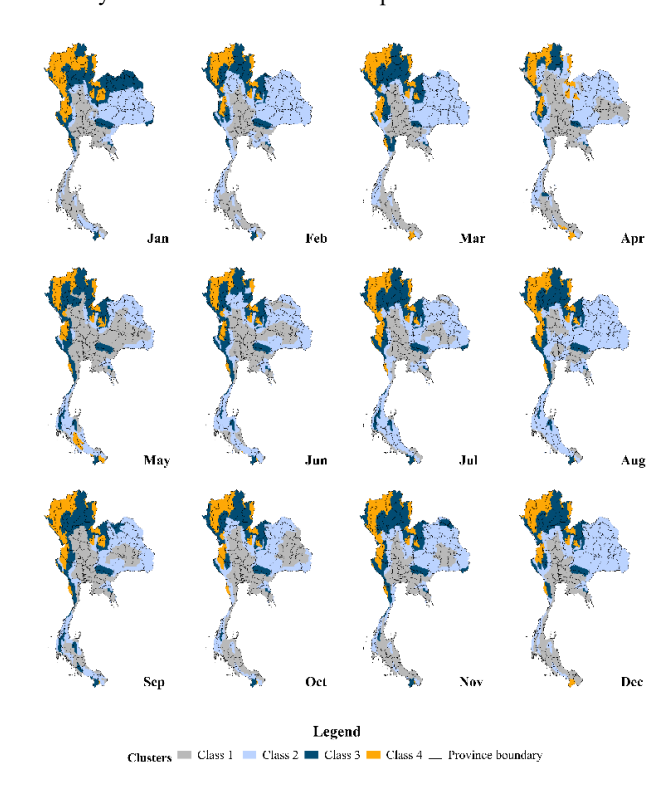


Figure 2. Spatial distribution of geographic-airshed clusters for each month

# 5.2 Seasonal Changes in Airshed Zoning

Monthly maps of the K-means output reveal a coherent, elevation-ordered pattern of "airshed clusters" across Thailand. Cluster 1 (Lowland) dominates the Central Plains, lower Northeast, and coastal deltas year-round; Cluster 4 (Highland) is concentrated along the northern and western ranges and parts of the Tenasserim Hills; Clusters 2–3 (Transition Zones 1–2) occupy foothills, plateau margins, and basin rims (e.g., around Chiang Mai–Lamphun and the Khorat Plateau). Spatial boundaries shift modestly with season, but the rank ordering of clusters by topography and atmosphere is persistent across months.

Variable	Airshed Cluster Level			
	Cluster 1	Cluster 2	Cluster 3	Cluster 4
DEM (m)	27.89	177.61	435.47	808.94
PBL (hPa)	556.08	488.48	434.99	427.62
PPT (mm)	174.36	154.87	133.94	113.59
SRAD (W/m <sup>2</sup> )	218.31	218.96	214.92	211.65
SUR (hPa)	1006.54	988.1	960.09	934.19
TMAX (°C)	32.37	31.84	31.41	30.12
TMIN (°C)	23.8	22.04	20.43	18.73
VAP (kPa)	2.93	2.62	2.44	2.2
WS (m/s)	1.84	1.41	1.21	1.28

Table 1. Summary of mean values for topographic and meteorological variables across the four clusters.

Cluster-means highlight systematic gradients that underpin these maps. Mean elevation rises monotonically from Cluster 1 to 4 ( $\approx\!28~\text{m}\to\approx\!809~\text{m}$ ), while surface pressure declines accordingly ( $\approx\!1006~\text{hPa}\to\approx\!934~\text{hPa}$ ). Air temperature follows the lapse-rate expectation: TMAX decreases by roughly 2.3 °C and TMIN by  $\approx\!5.1$  °C between lowland and highland clusters, indicating cooler nights and narrower diurnal ranges aloft. Atmospheric moisture proxies also decline with altitude; vapor pressure (VAP) drops by  $\approx\!0.7~\text{kPa}$ , consistent with drier boundary-layer conditions in uplands. Mean wind speed (WS) is highest in lowlands ( $\approx\!1.84~\text{m}~\text{s}^{-1}$ ) and lower in transitional/highland zones ( $\approx\!1.2{-}1.3~\text{m}~\text{s}^{-1}$ ), suggesting greater stagnation potential where terrain sheltering is stronger.

Two variables speak directly to dispersion capacity. First, PBL pressure decreases from  $\approx\!556$  hPa (Cluster 1) to  $\approx\!428$  hPa (Cluster 4), reflecting a systematically higher PBL-top altitude over high terrain and a thinner column above the surface—an important control on vertical mixing. Second, shortwave radiation (SRAD) is modestly lower in highlands ( $\approx\!212$  W m $^{-2}$ ) than in lowlands ( $\approx\!218$  W m $^{-2}$ ), consistent with cooler, cloudier, orographically influenced conditions that can suppress convective growth on some days. Together with weaker winds, these differences help explain the observed tendency for transition and basin-rim zones to experience stagnant episodes in the cool/dry season.

Seasonality is evident in the monthly cluster mosaics. From November to February, highland and transition classes expand and encroach farther into adjacent basins, coincident with lower temperatures and frequent stability. During the Southwest monsoon (May–October), transitional zones retract in many windward areas, and lowland extents stabilize, reflecting stronger synoptic ventilation and precipitation scavenging. This seasonal breathing of boundaries is most visible along mountain–valley interfaces in the North and along the western

cordillera. Despite these shifts, cluster identity at any given location is highly repeatable: most provinces remain in the same class or oscillate between a base class and its immediate neighbor (e.g.,  $2 \leftrightarrow 3$ ), supporting the idea of stable geoclimatic regimes with seasonal modulation.

Precipitation totals mirror the topographic ordering in this dataset ( $\approx$ 174 mm in lowlands to  $\approx$ 114 mm in highlands for monthly modes), reinforcing that the identified clusters capture not only thermal and dynamical structure but also hydrological regimes. The joint behavior of DEM, PBL, SRAD, SUR, TMAX/TMIN, VAP, WS, and PPT confirms that the four clusters are physically interpretable "airshed environments": (1) warm, moist, better-ventilated lowlands; (2–3) topographic transition belts with elevated stagnation risk; and (4) cool, drier highlands with distinct vertical structure. These results provide a reproducible basis for airshed-aware management, including seasonal targeting of monitoring and interventions in transition belts and basin interiors where stagnation and pollution accumulation are most likely.

### 5.3 Future Airshed Zoning Developing

To strengthen the physical basis of the zoning, a subsequent revision will incorporate explicit airflow diagnostics alongside DEM and meteorology. First, ventilation capacity (VC) will be computed as VC=WS10×PBLH, where WS10 is 10-m wind speed and PBLH is planetary boundary-layer height. Higher VC denotes greater flushing potential and lower risk of pollutant build-up. Second, stagnation frequency will be quantified as the monthly fraction of days meeting low-dispersion criteria (e.g., WS10 < 1.5 m s<sup>-1</sup>, PBLH < 500 m, and precipitation < 1 mm), with thresholds calibrated to regional conditions. These metrics will be aggregated to OBC segments and co-analyzed with existing predictors to refine boundaries and identify persistent accumulation belts.

Methodological transparency and validation will also be expanded. Because the present version prioritizes integrative mapping, several elements are under-specified and will be added: (i) choice of K reported with Elbow, Silhouette, and Gap statistics (using a one-SE rule); (ii) stability analysis via bootstrap resampling with Adjusted Rand Index summaries; and (iii) external/temporal holdouts, including independent PM2.5—based external checks, year-wise temporal splits, and leave-one-province-out spatial holdouts. These steps will document the robustness of cluster membership, quantify sensitivity to perturbations, and link regimes to observed pollution patterns across seasons.

Together, the airflow metrics (VC, stagnation frequency) and the expanded validation suite are expected to (a) align "airshed" delineation more tightly with dispersion capacity, (b) provide reproducible diagnostics for selecting K and assessing stability, and (c) yield policy-relevant thresholds (e.g., low-VC/high-stagnation alerts) for seasonal targeting of monitoring and interventions. These additions are planned for a subsequent revision given current time constraints.

# 6. Conclusion

This study delineated Thailand's airshed regimes by integrating topography with multi-variable meteorology in an object-based, K-means framework applied to monthly composites for 2003–2024. Guided by Elbow diagnostics, four physically interpretable clusters emerged—lowland, two transition belts, and highland—arranged monotonically by elevation and

accompanied by coherent gradients in surface pressure, temperature, moisture proxies, wind speed, shortwave radiation, and planetary boundary-layer (PBL) structure. Cluster means show declining surface pressure and cooling (both TMAX and TMIN) with altitude, alongside reductions in vapor pressure and precipitation; winds are generally stronger in lowlands and weaker in transition/highland zones. Lower PBL pressure in highland settings (indicative of higher PBL tops) and modestly reduced shortwave radiation together help explain a heightened propensity for stagnant conditions in basin rims and foothills during the cool/dry season.

Seasonality is pronounced yet systematic. From November to February, transition and highland classes expand into adjacent basins, consistent with lower temperatures and more frequent static stability; during the Southwest monsoon (May–October), transition belts retract in windward sectors as synoptic ventilation and wet scavenging strengthen. Despite these "breathing" boundaries, cluster identity at fixed locations is highly repeatable, indicating stable geoclimatic regimes modulated by seasonal forcing. This persistence suggests the clusters offer a reproducible spatial scaffold for air-quality management that respects physical, rather than administrative, boundaries.

The zoning has immediate operational relevance. First, it enables seasonally targeted interventions: densifying monitoring and issuing advisories in transition belts and basin interiors where stagnation risk is elevated, particularly during November–February. Second, it provides a common spatial language for cross-provincial coordination, aligning surveillance, emission controls, and public communication with shared dispersion environments. Third, the regimes can be incorporated into forecasting and early-warning systems (e.g., regime-conditioned thresholds for PM2.5), potentially improving lead time with minimal additional data requirements.

Several limitations bound these conclusions. The present delineation is dispersion-focused: it does not explicitly model emissions, chemical transformation, or long-range transport, and it emphasizes monthly modes rather than extremes. Reliance on gridded products introduces resolution and bias uncertainties, and coastal/complex terrain may require finer-scale wind and land–sea-breeze diagnostics. In addition, aspects of methodological transparency—choice of K, stability under resampling, and external/temporal holdouts—remain under-specified in the current version.

Planned extensions will address these gaps. We will incorporate explicit airflow diagnostics, namely ventilation capacity (VC = WS10  $\times$  PBLH) and stagnation frequency (share of days meeting low-dispersion criteria), aggregate them to object level, and re-evaluate cluster structure and boundaries. Validation will be expanded to include Elbow/Silhouette/Gap (with a one-SE rule), bootstrap stability via Adjusted Rand Index, and external/temporal holdouts using independent PM2.5 observations. These enhancements will further align the zoning with the physical drivers of accumulation and ventilation, strengthening its utility for seasonally adaptive, cross-boundary air-quality management.

### Acknowledgements

This research was funded by the National Research Council of Thailand for the year 2024 under the project "The Spatio-Temporal Analysis of Air Pollution Zones Using Geoinformatic technology"

### References

IQAir, 2023. 2023 World Air Quality Report. IQAir. iqair.com/world-air-quality-report (24 August 2025).

OPDC, 2019. Air Quality Management in Thailand. Office of the Pollution Control Department, Bangkok, Thailand.

Khan, A., et al., 2024. Airshed delineation for effective air quality management. *Atmospheric Environment*, 245, 118–129.

Ghosh, P., et al., 2021. Air pollution and public health: a review. *Environmental Science & Technology*, 53(5), 2345–2356.

Thitaporn, S., 2013. Air quality monitoring in Thailand: challenges and opportunities. *Journal of Environmental Management*, 45(3), 123–135.

Pope, C.A., et al., 2009. Health effects of particulate air pollution. *Annals of Epidemiology*, 19(4), 257–263. doi.org/10.1016/j.annepidem.2009.01.018.

Lelieveld, J., et al., 2015. The contribution of outdoor air pollution to premature mortality. *Nature*, 525, 367–371.

WHO, 2016. WHO Global Air Quality Guidelines: Particulate Matter (PM2.5 and PM10), Ozone, Nitrogen Dioxide, Sulfur Dioxide and Carbon Monoxide. World Health Organization, Geneva. who.int/publications/i/item/9789240034433 (24 August 2025).

Phopsuk, J., 2019. Air quality monitoring in Chiang Mai: a case study. Chiang Mai University Press, Chiang Mai, Thailand.

TDRI, 2024. Air pollution in Thailand: policy challenges and recommendations. Thailand Development Research Institute, Bangkok, Thailand.

Crippen, R.E., et al., 2016. Digital elevation models: a review. *Remote Sensing of Environment*, 176, 1–16.

Simiu, E., et al., 2015. Planetary boundary layer heights and their implications for air quality. *Atmospheric Environment*, 120, 1–10.

Abatzoglou, J.T., Dobrowski, S.Z., Parks, S.A., Hegewisch, K.C., 2018. TerraClimate: a high-resolution global dataset of monthly climate and climatic water balance from 1958–2015. *Scientific Data*, 5, 170191. doi.org/10.1038/sdata.2017.191.

Araghi, A., Martinez, C.J., Adamowski, J.F., 2023. Evaluation of TerraClimate gridded data in investigating the changes of reference evapotranspiration in different climates of Iran. *Theoretical and Applied Climatology*, 132(3–4), 1027–1042. doi.org/10.1007/s00704-023-03986-1.

Royal Irrigation Department, 2014. Annual Report 2014. Ministry of Agriculture and Cooperatives, Bangkok, Thailand. dl.parliament.go.th/handle/20.500.13072/518600 (24 August 2025).

Saldanha, R., et al., 2024. Advancements in air quality monitoring technologies. *Environmental Monitoring and Assessment*, 196(4), 129.

Hall, D.B., Minns, A.W., 1999. K-means clustering for environmental data. *Environmental Modelling & Software*, 14(3), 227–236.

Wang, Z., 2018. Eco-region delineation using object-based image analysis (OBIA) and climate datasets. M.S. thesis, Department of Geography, The Ohio State University, Columbus, OH, USA.